

### **Responses to Referee #1:**

This paper studied the chemical compositions and mixing states of single particles in a rural site in the southeastern margin of the Tibetan Plateau (TP). The major particle types and size distributions of single particles were discussed, and the results of backward trajectories were coupled to investigate the regional impact on the formation of single particles in the sampling site. Two episodes were selected to discuss the transport and secondary formation processes of single particles. In addition, the linear regressions between several marker ions and RH,  $O_x$  were explored to elucidate the formation processes of these secondary species. Generally, in view of the lack of field observation data in Tibetan Plateau, this study provides a good opportunity to investigate the mixing states and formation processes of single particles, which is of great significance to evaluate the influence of fine particles on the climate change in TP. However, several issues need to be addressed and some revisions are necessary before the acceptance of this manuscript.

**Response:** We highly appreciate the thoughtful and valuable suggestions by the reviewer, which are helpful for us to improve the quality of our manuscript. We have carefully addressed the comments in point-by-point form as shown below. Detailed responses to the comment are highlighted in blue, and the revised text is underlined in italics. Attached please also find the marked-up manuscript with tracked changes in the revised manuscript.

1. The size distributions of single particles from SPAMS should be scaled by other instruments such as SMPS, otherwise, the unscaled size distributions of single particles should be treated carefully, which mainly referred to the relative changes of same type particles at different period. The comparison of different type particles and quantitative description of size patterns are usually inaccurate. Authors presented many results of size distributions, but the length of discussions should be reduced and some expressions should be revised.

**Response:** Thank you for pointing out the unsuitable comparison. After considering the comments, we simplified the description of particle size distribution. As shown in Section 3.2 (new Lines 270-297), we also reduced the comparison and quantitative descriptions of the size distribution of different types of particles, due to their scales were not fully adjusted with either instruments or sampling periods. Those changes can be seen in the revised manuscript with “tracked change”. Besides, due to the substantial changes that have been made, all the revisions have not been shown here, but the critical ones are listed as below.

Section 3.2 in Lines 270-297:

*“The aerodynamic size distributions of all particle types are shown in Fig. 3. According to the characteristics of the average MS (Text S1 and Fig. S3), rich-K, BB, OC and EC-aged particles originated from the similar sources of*

vehicle emission or solid-fuel combustion. Their size distribution thus presents within a small-scale (~440 nm) (Fig. 3a). However, the relative percentage of each particle type is distinct with different size ranges, possibly due to the unique atmospheric processing. For example, as shown in Fig. 3b, the proportions of rich-K and BB types increase along with the increases in particle size from 200 to 420 nm but then decrease. OC and EC-aged types are mainly distributed in relatively small particle sizes, and their proportions gradually decrease when the size ranges become larger. Ammonium and Dust types are mainly distributed in large sizes of ~600 nm (Fig. 3a). The proportion of Ammonium particles gradually increases with the increase of particle size and peaks at 740 nm, the relatively large size distribution is ascribed to the intense atmospheric aging during regional transport (Text S1). The proportion of Dust particles gradually increases with a size > 560 nm and peaks at 1.48  $\mu\text{m}$ . This is consistent with the fact that dust is a coarse particle, generally formed at the roadside and fly ash.

Compared with the total particle size distribution, the peak values of the six main particle types show minor differences (< 80 nm) during the two different episode periods (Fig. S10a). In Fig. S10b, a relatively high proportion of the rich-K and BB particles exhibit bimodal distributions, while peaks at < 300 nm are affected by the primary emissions and > 300 nm are associated with the aging process (Li et al., 2022b; Bi et al., 2011). Hence, the percentage of the six particle types distribute in wider size ranges during E2 than E1 due to the more intensive atmospheric aging. Relatively greater fluctuation for the large-size fractions (> 1.1  $\mu\text{m}$ ) could be explained by the low particle concentration (a number less than 20). It should be pointed out that further application of this method would require a co-located particle-sizing instrument to scale the size-resolved particle detection efficiency. Both particle composition and size-dependent are the predominant impacting factors on the particle detection efficiency of the SPAMS (Wenzel et al., 2003; Yang et al., 2017; Healy et al., 2013).”

2. Line 32-33: why the volatilization of nitrate would lead to more abundant of sulfate?

**Response:** Sorry for the confusion. Our original statement aims to describe that the more volatilized nitrate ( $^{62}\text{NO}_3^-$ ) leads to the low mixing of nitrate in the TP particles during the transport process. In contrast to nitrate, less volatilized sulfate mixes with the TP particles. The statement has been revised as follows.

Line 32-34

“Compared with the abundant sulfate ( $^{97}\text{HSO}_4^-$ ), the low nitrate ( $^{62}\text{NO}_3^-$ ) internally mixed in TP particles is mainly due to the fact that nitrate is more volatilized during the transport process.”

3. Line 34-35: not all of these secondary species showed strong linear regressions with RH and Ox from the discussion of Section 3.3. Authors should give a more precise conclusion.

**Response:** Suggestion taken. A detailed description of the formation mechanism of secondary species is shown in Section 3.3. The linear regressions between each secondary species and  $O_x$  are different during E1 and E2. The number fractions of these secondary species have moderate to strong positive correlations with RH during the two episodes, except that  $^{43}\text{C}_2\text{H}_3\text{O}^+$  during E2 and  $^{89}\text{HC}_2\text{O}_4^-$  during E1. Furthermore,  $^{62}\text{NO}_3^-$  has an insignificant correlation with RH during E1 and presents a moderate negative correlation with RH during E2. Conclusively, the formation capacity of atmospheric oxidation is presumably weakened by the convective transmission and strengthened by the regional transport in TP, but RH could significantly promote the formation of secondary species, especially  $^{97}\text{HSO}_4^-$  and  $^{18}\text{NH}_4^+$ . The sentence has been rewritten in the Abstract as follows.

Line 34-38

*“The formation mechanism of secondary speciation demonstrates that the formation capacity of atmospheric oxidation is presumably affected by the convective transmission and the regional transport in TP. However, the relative humidity (RH) could significantly promote the formation of secondary species, especially for  $^{97}\text{HSO}_4^-$  and  $^{18}\text{NH}_4^+$ .”*

4. Many field studies via SPAMS have been reported in recent years, thus, authors should add some new references especially those published after 2018.

**Response:** Thanks for pointing out these. We have replaced the old references with more updated ones. For example, in Lines 91-96, new references are added as follows.

Line 91-96:

*“At the same time, aerosol time-of-flight mass spectrometry (ATOFMS) (Dall’Osto et al., 2014) and single particle aerosol mass spectrometer (SPAMS) (Zhang et al., 2020) are popular for characterizing atmospheric individual particles. These devices can determine the chemical compositions and size distributions of the particles in detail, such as the dynamic processes of chemical aging, mixing state, and transport of the aerosols (Liang et al., 2022; Li et al., 2022b; Zhang et al., 2019b).”*

#### **References:**

Li L., Wang, Q. Y., Zhang, Y., Liu, S. X., Zhang, T., Wang, S., Tian, J., Chen, Y., Hang Ho, S. S., Han, Y., and Cao, J.J.: Impact of reduced anthropogenic emissions on chemical

characteristics of urban aerosol by individual particle analysis, *Chemosphere*, 303, 135013, <https://doi.org/10.1016/j.chemosphere.2022.135013>, 2022b.

Liang, Z. C., Zhou, L. Y., Cuevas, R. A., Li, X. Y., Cheng, C. L., Li, M., Tang, R. Z., Zhang, R. F., Lee Patrick K. H., Lai, Alvin C. K., and Chan, C.K.: Sulfate Formation in Incense Burning Particles: A Single-Particle Mass Spectrometric Study, *Environ. Sci. Technol. Lett.*, 9, 718–725, <https://doi.org/10.1021/acs.estlett.2c00492>, 2022.

Zhang, G. H., Lin, Q. H., Peng, L., Yang, Y. X., Jiang, F., Liu, F. X., Song, W., Chen, D. H., Cai, Z., Bi, X. H., Miller, M., Tang, M. J., Huang, W. L., Wang, X. M., Peng, P. A., Shen, G. Y.: Oxalate Formation Enhanced by Fe-Containing Particles and Environmental Implications, *Environ. Sci. Technol.*, 53, 1269–1277, <https://doi.org/10.1021/acs.est.8b05280>, 2019b.

Zhang, G. H., Lian, X. F., Fu, Y. Z., Lin, Q. H., Li, L., Song, W., Wang, Z. Y., Tang, M. J., Chen, D. H., Bi, X. H., Wang, X. M., and Sheng, G. Y.: High secondary formation of nitrogen-containing organics (NOCs) and its possible link to oxidized organics and ammonium, *Atmos. Chem. Phys.*, 20, 1469–1481, <https://doi.org/10.5194/acp-20-1469-2020>, 2020.

5. There are many grammatical errors and unprofessional descriptions in the manuscript, such as: line 47-48, “making their impact on the air more uncertain”; line 74-75, “Atmospheric aerosols also can influence the properties and life span of clouds as cloud condensation nuclei”; line 81, “Most studies have focused on the influence of optical properties”; line 92, “with a high temporal resolution”; line 95, “AMS/ACSM mainly used to provide”; line 102, remove “full” from “determine the full chemical composition”; line 107, “The shortage of information”; line 115, “pre-monsoon, to continuously (i) investigate”; line 123, “2.1 Observation site”; line 129, “The villagers make a living by farming (e.g., potato and autumn rape), and biomass is the main residential fuel”; line 143, “a detection moment”; line 194, “Differently, few”. In general, the related grammatical errors are not limited to these examples, authors should carefully revise the manuscript to meet the quality of ACP.

**Response:** Thanks for pointing out the mistakes. The revised manuscript has been edited and proofread by a native English speaker. All related grammatical errors shown in this comment have been corrected as follows.

Line 47-49:

*“After further coating through coagulation, condensation and photochemical oxidation, its sizes, chemical compositions, mixing states, and optical properties would change greatly, leading to its influence in the atmosphere more uncertain”*

Line 68-70:

*“Atmospheric aerosols also can act as cloud condensation nuclei to impact the local hydrological cycles and monsoon patterns by changing the microphysical properties and life span of clouds.”*

Line 73-75:

*“Most studies have focused on the optical characteristics within the TP; however, only a few research has been conducted on aerosol components.”*

Line 85:

*“More advanced aerosol online measurement equipment with high-time resolution....”*

Line 85-91:

*“More advanced aerosol online measurement equipment with high-time resolution, such as the aerosol chemical speciation monitor (ACSM) and aerosol mass spectrometer (AMS) (Ng et al., 2011; Canagaratna et al., 2007) are mainly used to achieve online observation datasets of non-refractory submicron aerosol (including the mass concentration of sulfate, nitrate, ammonium, chloride, and organic; and their corresponding mass spectral). This is beneficial to recognize the dynamic processes of source emission in the atmosphere (Du et al., 2015; Zhang et al., 2019a).”*

Line 93-96:

*“These devices can determine the chemical composition and size distribution of the particles in detail, such as the dynamic processes of chemical aging, mixing state, and transport of the aerosols (Liang et al., 2022; Li et al., 2022b; Zhang et al., 2019b).”*

Line 96-100:

*“To the best knowledge, the advanced measurement device has not yet been applied for the studies conducted in TP, leading to a lack of in-depth research on the PM<sub>2.5</sub> pollution in TP, especially in the southeastern margin, which hinders our understanding of the distribution characteristics and formation mechanism of aerosol components in high-altitude regions.”*

Line 104-106:

*“In this study, continuous field observation of individual particles (SPAMS) was deployed on the southeastern margin of the TP during the pre-monsoon period, to (i) investigate...”*

Line 113:

*“2.1 Sampling site”*

Line 119-120:

*“Villagers earn a living by farming (e.g., potato and autumn rape), and biomass is the major domestic fuel (Li et al., 2016).”*

Line 133-135:

*“In summary, a velocity, a detection time, and an ion mass spectrum are recorded for each ionized particle, while there is no mass spectrum for not ionized particles.”*

Line 187-190:

*“The difference is that few researchers can capture the high proportion of Ammonium particles as shown in this study (Shen et al., 2017; Xu et al., 2018), which is ascribed to the conversion of ammonia (NH<sub>3</sub>) precursor emitted from large-scale agricultural activities and mountain forest (Engling et al., 2011; Li et al., 2013).”*

6. Line 49-59: these sentences in the introduction were repetitive and should be reduced in length.

**Response:** We agreed with this point. The statements have been revised as follows.

Line 47-54:

*“After further coating through coagulation, condensation and photochemical oxidation, its sizes, chemical compositions, mixing states, and optical properties would change greatly, leading to its influence in the atmosphere more uncertain (Jacobson, 2002; Zaveri et al., 2010; Matsui, 2016; Budisulistiorini et al., 2017; Ma et al., 2012). Currently, the influences of the complex chemical components on aerosol size and mixing state show large regional differences due to the variations in the pollution sources, atmospheric formation mechanism and meteorological conditions, which have been widely studied in an urban area at a low altitude (Pratt et al., 2011; Liu et al., 2020a; Xu et al., 2017; Wang et al., 2022).”*

**Reference:**

Xu, J., Li, M., Shi, G., Wang, H., Ma, X., Wu, J., Shi, X., and Feng, Y.: Mass spectra features of biomass burning boiler and coal burning boiler emitted particles by single particle aerosol mass spectrometer, *Sci. Total Environ.*, 598, 341–352, <https://doi.org/10.1016/j.scitotenv.2017.04.132>, 2017.

7. Line 94-95: The AMS and SPAMS both have its advantages to conduct the researches in aerosols, so you can directly present their application in the aerosol study instead of pointing out the things they can't do.

**Response:** The description of the AMS/ACSM deficiencies has been deleted. Their application in the aerosol study has been added to the revised manuscript. We have rewritten this text as follows.

Line 85-91:

*“More advanced aerosol online measurement equipment with high-time resolution, such as the aerosol chemical speciation monitor (ACSM) and aerosol mass spectrometer (AMS) (Ng et al., 2011; Canagaratna et al., 2007) are mainly used to achieve online observation datasets of non-refractory submicron aerosol (including the mass concentration of sulfate, nitrate, ammonium, chloride, and organic; and their corresponding mass spectra). This is beneficial to recognize the dynamic processes of source emission in the atmosphere (Du et al., 2015; Zhang et al., 2019a).”*

8. Line 165-168: the “Aging Element Carbon (EC-aged)” should be “aged elemental carbon (EC-aged)” . “Potassium-containing (NaK-SN),” doesn’ t match its abbreviation, and what is the difference of this type with “Potassium-rich (rich-K)” ?

**Response:** We do apologize for the unclear description of the “NaK-SN” particles in the original manuscript. Particles containing the strongest  $K^+$  ( $m/z$   $^{39}K^+$ ) signal accompanies by a significant sulfate signal ( $m/z$   $^{97}HSO_4^-$ ) in positive MS, and nitrate signals ( $m/z$   $^{46}NO_2^-$ ,  $^{62}NO_3^-$ ) in the negative MS, are identified as Potassium-rich (rich-K) (Fig. S3a). Compared with the rich-K particles, the NaK-SN particles also contain abundant sodium ion signal in the positive MS, but more abundant with sulfate shown in the negative MS. In addition, the intensities of nitrate fragments are significantly lower. Considering such differences between rich-K and NaK-SN particles, they might come from unique origins (e.g., sources and distribution characteristics). Therefore, the two particle types are resolved separately. The statements have been revised as below.

Line 157-161:

*“Finally, eight major particle clusters [i.e., potassium-rich (rich-K), biomass burning (BB), organic carbon (OC), Ammonium, aged element carbon (EC-aged), Dust, sodium (Na)-potassium (K)-containing (NaK-SN), and iron (Fe)-lead (Pb)-containing (Metal)] with distinct chemical patterns were manually combined, which represent ~99.7 % of the population of the detected particles.”*

9. Line 177: For the trajectory clusters analysis, I don’t think the height of 500 m is reasonable to elucidate the transportation of air masses in consideration of the mountains and plateau surrounding the sampling site.

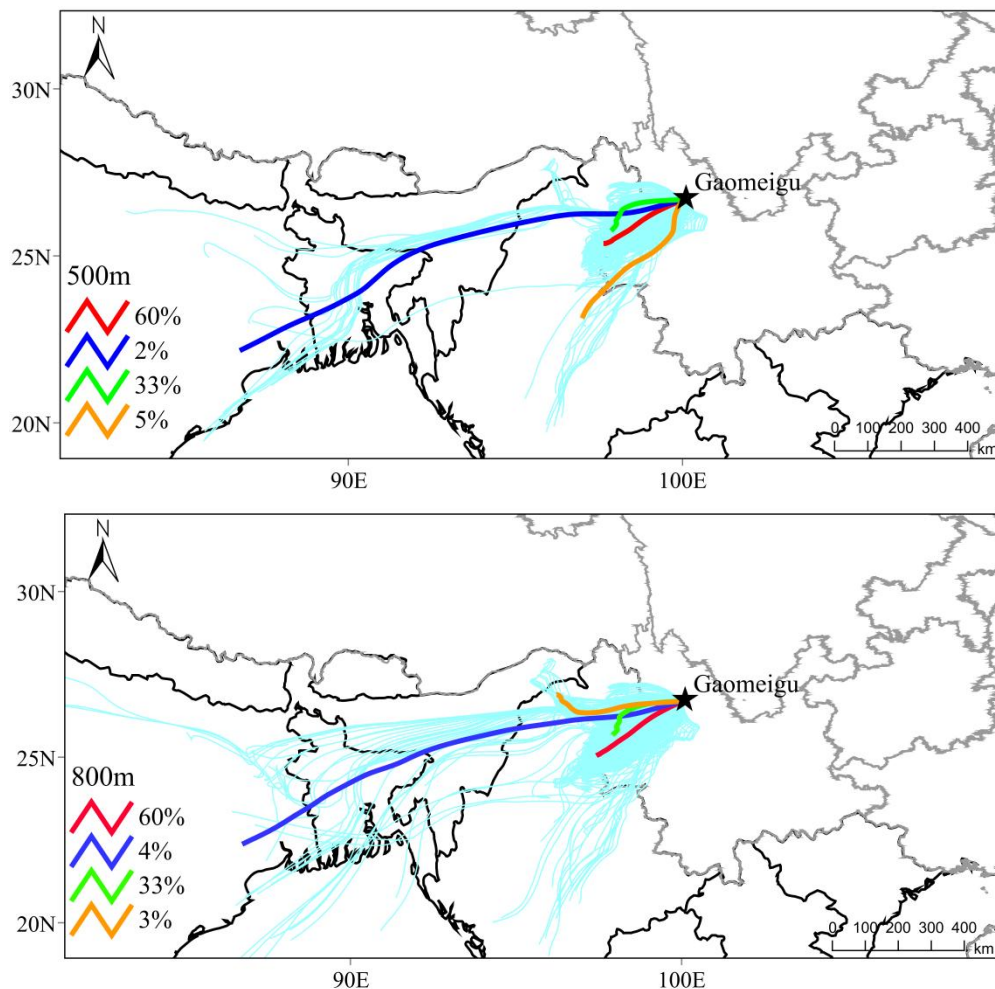
**Response:** HYSPLIT converts the vertical layers from the original coordinate system into its terrain-following coordinate system (sigma) and directly uses the data contained in meteorological files to the calculated trajectory (Draxler and Hess, 1998). GDAS data is derived from the sigma coordinate as well. The surface in the terrain-following coordinate system is consistent with the coordinate surface, so solves the problem of modeling near mountains area (Phillips, 1965). The trajectory position could be slightly different because of using different meteorological files



which origin from the data discrepancy in the different meteorological files, but this method has been used over complex terrain with various meteorological data (Khan et al., 2010; Burley and Bytnerowicz 2011; Qu et al 2015; Wang et al., 2015, 2019).

To further determine if the trajectory would be impacted by the surface rising. We have performed sensitivity tests for the starting height. Fig. R1 show the 72-h backward trajectories based on the assumed starting height of 800 m and 1000 m, respectively. Although there is some difference in the 72-h backward trajectories between the three different heights (i.e., 500, 800 and 1000 m), the main transport pathways are similar. We finally ran the trajectory at 500 m is considerably representative of the average planetary boundary level (~590 m). This has been also adopted in many other studies (Zhang et al., 2019; Lu et al., 2012; Liu et al., 2021; Tian et al., 2023).

Four groups of air masses are identified based on their transport pathways (Fig. R1). The maps show that the major trajectory clusters are similar at different arrival heights, representing that the height of 500 m could effectively capture the large-scale flow patterns.





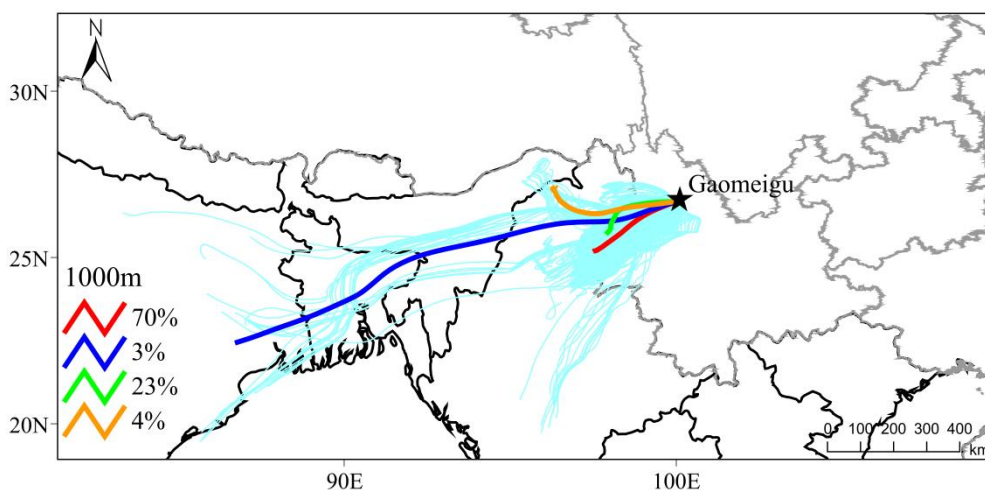


Figure R1. Maps of mean trajectory clusters at arrival heights of 500, 800, and 1000 m above ground level during the campaign.

### References:

- Burley, J. D., and Bytnerowicz, A.: Surface ozone in the White Mountains of California, *Atmospheric Environment*, 45, 4591 – 4602, <https://10.1016/j.atmosenv.2011.05.062>, 2011.
- Draxler, R. and Hess, G.: An overview of the HYSPLIT\_4 modelling system for trajectories, *Aust. Meteorol. Mag.*, 47, 295–308, 1998.
- Khan, A. J., Li, J. J., Dutkiewicz, V. A., and Husain, L.: Elemental carbon and sulfate aerosols over a rural mountain site in the northeastern United States: Regional emissions and implications for climate change, *Atmos. Environ.*, 44, 2364–2371, <https://10.1016/j.atmosenv.2010.03.025>, 2010.
- Lu, Z. F., Streets, D.G., Zhang, Q., and Wang, S.W.: A novel back-trajectory analysis of the origin of black carbon transported to the Himalayas and Tibetan Plateau during 1996–2010, *Geophys. Res. Lett.*, 39, L01809, <https://doi.org/10.1029/2011GL049903>, 2012.
- Phillips, N. A.: A coordinate system having some special advantages for numerical forecasting, *Shorter contributions, J. Atmos. Sci.*, 14, 184–185, 1957.
- Qu, C. K., Xing, X. L., Albanese, S., Doherty, A., Huang, H. F., Lima, A., Qi, S. H., and De Vivo, B.: Spatial and seasonal variations of atmospheric organochlorine pesticides along the plain-mountain transect in central China: Regional source vs. long-range transport and airsoil exchange, *Atmos. Environ.*, 122, 31–40, <https://doi.org/10.1016/j.atmosenv.2015.09.008>, 2015.
- Liu, H. K., Wang, Q. Y., Xing, L., Zhang, Y., Zhang, T., Ran, W. K., and Cao, J. J.: Measurement report: quantifying source contribution of fossil fuels and biomass-burning black carbon aerosol in the southeastern margin of the Tibetan Plateau, *Atmos. Chem. Phys.*, 21, 973–987, <https://doi.org/10.5194/acp-21-973-2021>, 2021.
- Tian, J., Wang, Q. Y., Ma, Y. Y., Wang, J., Han, Y. M., and Cao, J. J.: Impacts of biomass burning and photochemical processing on the light absorption of brown carbon in the southeastern Tibetan Plateau, *Atmos. Chem. Phys.*, 23, 1879–1892, <https://doi.org/10.5194/acp-23-1879-2023>, 2023.
- Wang, Q. Y., Huang, R. J., Cao, J. J., Tie, X. X., Ni, H. Y., Zhou, Y. Q., Han, Y. M., Hu, T. F., Zhu, C. S., Feng, T., Li, N., and Li, J. D.: Black carbon aerosol in winter northeastern

Qinghai-Tibetan Plateau, China: the source, mixing state and optical property, *Atmos. Chem. Phys.*, 15, 13059–13069, <https://doi.org/10.5194/acp-15-13059-2015>, 2015.

Wang, Q. Y., Han, Y. M., Ye, J. H., Liu, S. X., Pongpiachan, S., Zhang, N. N., Han, Y. M., Tian, J., Wu, C., Long, X., Zhang, Q., Zhang, W. Y., Zhao, Z. Z., and Cao, J. J.: High contribution of secondary brown carbon to aerosol light absorption in the southeastern margin of Tibetan Plateau, *Geophys. Res. Lett.*, 46, 4962–4970, <https://doi.org/10.1029/2019GL082731>, 2019.

Zhang, X. H., Xu, J. Z., Kang, S. C., Zhang, Q., and Sun, J. Y.: Chemical characterization and sources of submicron aerosols in the northeastern Qinghai – Tibet Plateau: insights from high-resolution mass spectrometry, *Atmos. Chem. Phys.*, 19, 7897–7911, <https://doi.org/10.5194/acp-19-7897-2019>, 2019.

10. Line 190: May be the name of secondary type particles is more reasonable than the name of rich-K in Table 1.

**Response:** In many previous studies, the rich-K type is indeed named as a secondary related particle type (Bi et al., 2011; Chen et al., 2016, 2017; Shen et al., 2017). However, there are complicated sources of the rich-K type particles, including biomass burning, secondary formation, and industrial and traffic emissions (Pratt et al., 2011; Bi et al., 2011; Shen et al., 2017; Zhang et al., 2017). In this study, a weak phosphate ( $m/z$   $^{79}\text{PO}_3^-$ ) signal in the average mass spectra (Fig. S3a) implies that the rich-K type might be affected by vehicle emissions (Yang et al., 2017). Although significant signals of  $^{97}\text{HSO}_4^-$  and  $^{62}\text{NO}_3^-$  indicate that the rich-K type might also experience atmospheric aging after the primary emission, the naming of “rich-K particles” as “secondary type particles” would lead to the misunderstanding that the rich-K particle would only be formed by secondary reactions.

#### References:

- Bi, X. H., Zhang, G. H., Li, L., Wang, X. M., Li, M., Sheng, G. Y., Fu, J. M., and Zhou, Z.: Mixing state of biomass burning particles by single particle aerosol mass spectrometer in the urban area of PRD, China, *Atmos. Environ.*, 45, 3447–3453, <https://doi.org/10.1016/j.atmosenv.2011.03.034>, 2011.
- Chen, Y., Cao, J. J., Huang, R. J., Yang, F. M., Wang, Q. Y., and Wang, Y. C.: Characterization, mixing state, and evolution of urban single particles in Xi’an (China) during wintertime haze days, *Sci. Total Environ.*, 573, 937–945. <http://dx.doi.org/10.1016/j.scitotenv.2016.08.151>, 2016.
- Chen, Y., Wenger, J. C., Yang, F. M., Cao, J. J., Huang, R. J., Shi, G. M., Zhang, S. M., Tian, M., and Wang, H. B.: Source characterization of urban particles from meat smoking activities in Chongqing, China using single particle aerosol mass spectrometry, *Environ. Pollut.*, 228, 92–101, <http://dx.doi.org/10.1016/j.envpol.2017.05.022>, 2017.
- Pratt, K. A., Murphy, S. M., Subramanian, R., DeMott, P. J., Kok, G. L., Campos, T., Rogers, D. C., Prenni, A. J., Heymsfield, A. J., Seinfeld, J. H., and Prather, K. A.: Flight-based chemical characterization of biomass burning aerosols within two prescribed burn smoke plumes, *Atmos. Chem. Phys.*, 11, 12549–12565, <https://doi.org/10.5194/acp-11-12549-2011>, 2011.

- Shen, L. J., Wang, H. L., Lü, S., Zhang, X. H., Yuan, J., Tao, S. K., Zhang, G. J., Wang, F., and Li, L.: Influence of pollution control on air pollutants and the mixing state of aerosol particles during the 2nd World Internet Conference in Jiaying, China, *J. Clean. Prod.*, 149, 436–447, <http://dx.doi.org/10.1016/j.jclepro.2017.02.114>, 2017.
- Yang, J., Ma, S. X., Gao, B., Li, X. Y., Zhang, Y. J., Cai, J., Li, M., Yao, L. A., Huang, B., and Zheng, M.: Single particle mass spectral signatures from vehicle exhaust particles and the source apportionment of on-line PM<sub>2.5</sub> by single particle aerosol mass spectrometry, *Sci. Total Environ.*, 593, 310–318, <https://doi.org/10.1016/j.scitotenv.2017.03.099>, 2017.
- Zhang, J. K., Luo, B., Zhang, J. Q., Ouyang, F., Song, H. Y., Liu, P. C., Cao, P., Schäfer, K., Wang, S. G., Huang, X. J., and Lin, Y. F.: Analysis of the characteristics of single atmospheric particles in Chengdu using single particle mass spectrometry, *Atmos. Environ.*, 157, 91–100, <https://doi.org/10.1016/j.atmosenv.2017.03.012>, 2017.

11. Line 199: Authors made a mistake here. [58C<sub>2</sub>H<sub>5</sub>NHCH<sub>2</sub>+] is not the marker of DEA, actually, the marker ion of DEA is [74H<sub>2</sub>NC<sub>4</sub>H<sub>10</sub>+]. Thus, the following discussions associated with DEA were incorrect in lines 200-208, 270-273.

**Response:** Thanks for the reminder. Although mass-to-charge ratio ( $m/z$ ) 58[C<sub>2</sub>H<sub>5</sub>NHCH<sub>2</sub>]<sup>+</sup> is identified as diethylamine (DEA) in many references (e.g., Lin et al., 2017), a more in-depth review of the literature show that  $m/z$  58[C<sub>2</sub>H<sub>5</sub>NHCH<sub>2</sub>]<sup>+</sup> is more reasonable to present as amine fragment (Moffet et al., 2008; Angelino et al., 2001; Silva et al., 2008), while  $m/z$  74[(C<sub>2</sub>H<sub>5</sub>)<sub>2</sub>NH<sub>2</sub>]<sup>+</sup> is diethylamine (DEA) (Healy et al., 2015; Chen et al., 2019; Cheng et al., 2018). Based on the reviewer’s comment, the marker ion of DEA is now identified as an amine fragment in this revised manuscript. And the related discussions on 58[C<sub>2</sub>H<sub>5</sub>NHCH<sub>2</sub>]<sup>+</sup> have been consequently modified as below.

Line 190-197:

*“It is necessary to point out that 60% of Ammonium particles contain signals of amine fragment ( $m/z$  58, C<sub>2</sub>H<sub>5</sub>NH=CH<sub>2</sub><sup>+</sup>), implying their similar formation pathway (Zhang et al., 2012). Moreover, the amine-containing particle contributes 12.5% of the total particles, which is significantly higher than that in some urban areas at low altitudes (~2% only) (Cahi et al., 2012; Zhang et al., 2015; Li et al., 2017) but is comparable to that at observed sites with high RH, or during fog and cloud events at a high altitude (>9%) (Roth et al., 2016; Lin et al., 2019).”*

Line 197-200:

*“This suggests that the formation of amines under high RH and fog conditions might exist in the Gaomeigu area (with an altitude of 3260 m), for example, the high relative fraction of amine-containing particle corresponds to a high RH (Fig. S4), and the existence of amine sources govern the ammonium formations (Bi et al., 2016; Rehbein et al., 2011).”*

Line 300-303:

*“The presences of amine ( $m/z$   $^{58}\text{C}_2\text{H}_5\text{NHCH}_2^+$ ) and sulfuric acid ( $m/z$   $^{195}\text{H}(\text{HSO}_4)_2^-$  signals are possibly indicative of the water uptake (Chen et al., 2019) and acidic property of the particles (Rehbein et al., 2011), respectively.”*

Line 311-313:

*“Meanwhile, relatively high number fractions of  $^{195}\text{H}(\text{HSO}_4)_2^-$  and  $^{58}\text{C}_2\text{H}_5\text{NHCH}_2^+$  are also observed in Ammonium (63% and 60%) and EC-aged (4% and 19%) particles.”*

Line 357-359:

*“The fractions of  $^{58}\text{C}_2\text{H}_5\text{NHCH}_2^+$  are significantly higher in E2 than E1 for Ammonium (67% versus 31%) and EC-aged particles (48% versus 17%), due to the relatively higher hygroscopic behavior (i.e., RHs) (Sorooshian et al., 2007).”*

## Reference:

- Angelino, S., Suess, D. T., and Prather, K. A.: Formation of aerosol particles from reactions of secondary and tertiary alkylamines: characterization by aerosol time-of-flight mass spectrometry, *Environ. Sci. Technol.*, 35, 3130–3138, <https://doi.org/10.1021/es0015444>, 2001.
- Chen, Y., Tian, M., Huang, R. J., Shi, G. M., Wang, H. B., Peng, C., Cao, J. J., Wang, Q. Y., Zhang, S. M., Guo, D. M., Zhang, L. M., and Yang, F. M.: Characterization of urban amine-containing particles in southwestern China: seasonal variation, source, and processing, *Atmos. Chem. Phys.*, 19, 3245–3255, <https://doi.org/10.5194/acp-19-3245-2019>, 2019.
- Cheng, C. L., Huang, Z. Z., Chan, C. K., Chu, Y. X., Li, M., Zhang, T., Ou, Y. B., Chen, D. H., Cheng, P., Li, L., Gao, W., Huang, Z. X., Huang, B., Fu, Z., and Zhou, Z.: Characteristics and mixing state of amine-containing particles at a rural site in the Pearl River Delta, China, *Atmos. Chem. Phys.*, 18, 9147–9159, <https://doi.org/10.5194/acp-18-9147-2018>, 2018.
- Healy, R. M., Evans, G. J., Murphy, M., Sierau, B., Arndt, J., McGillicuddy, E., O’ Connor, I. P., Sodeau, J. R., and Wenger, J. C.: Single-particle speciation of alkylamines in ambient aerosol at five European sites, *Anal. Bioanal. Chem.*, 407, 5899–5909, <https://doi.org/10.1007/s00216-014-8092-1>, 2015.
- Lin, Q. H., Zhang, G. H., Peng, L., Bi, X. H., Wang, X. M., Brechtel, F. J., Li, M., Chen, D. H., Peng, P. A., Sheng, G. Y., and Zhou, Z.: In situ chemical composition measurement of individual cloud residue particles at a mountain site, southern China, *Atmos. Chem. Phys.*, 17, 84730–84888, <https://doi.org/10.5194/acp-17-8473-2017>, 2017.
- Moffet, R. C., Foy, B. D., Molina, L. A., Molina, M. J., and Prather, K. A.: Measurement of ambient aerosols in northern Mexico City by single particle mass spectrometry, *Atmos. Chem. Phys.*, 8 (16), 4499–4516, <https://doi.org/10.5194/acpd-7-6413-2007>, 2008.

12. Line 215-217: how do you make sure the contribution of BB transport under the influence of PBL change?

**Response:** According to the descriptions in Text S1, the sources of the rich-K and OC particle types are biomass burning as well as traffic emission. Combining the results of Liu et al (2021), intensive contributions of biomass burning from upwind regions and of traffic emissions at two heavy highways are found. The increases in PBL height and wind speed lead to greater diffusion of air pollutants from the surroundings to the sampling site. Therefore, the particle types of rich-K, BB, and OC rapidly increase around 07:00 LT due to the enhanced emissions of biomass and traffic in the early morning. Revisions have been added as follows.

Line 207-211:

*“Then, their intensities rapidly increase in the morning (around 07:00 LT) due to more pollutants from biomass burning and traffic emissions at the upwind region, The increases of PBL height and WS also lead to the air pollutants transported from the surrounding environment to the sampling site (Liu et al., 2021).”*

### References:

Liu, H. K., Wang, Q. Y., Xing, L., Zhang, Y., Zhang, T., Ran, W. K., and Cao, J. J.: Measurement report: quantifying source contribution of fossil fuels and biomass-burning black carbon aerosol in the southeastern margin of the Tibetan Plateau, Atmos. Chem. Phys., 21, 973–987, <https://doi.org/10.5194/acp-21-973-2021>, 2021.

13. Line 223: “and road dust from upwind areas”, this is a contradictory expression.

**Response:** After consideration, the sentence has been changed as below.

Line 216-218:

*“After that, their levels continuously elevate until ~11:00 LT due to the regional transport, traffic emission, and fugitive dust (Text S2).”*

14. Line 230: “The most dominant air masses are Cluster 1, 3 and 4 from northeastern Myanmar”, actually, you only have four trajectories, so you cannot say three trajectories were dominant.

**Response:** According to the reviewer’s suggestion, the statement has been revised as below.

Line 224-225:

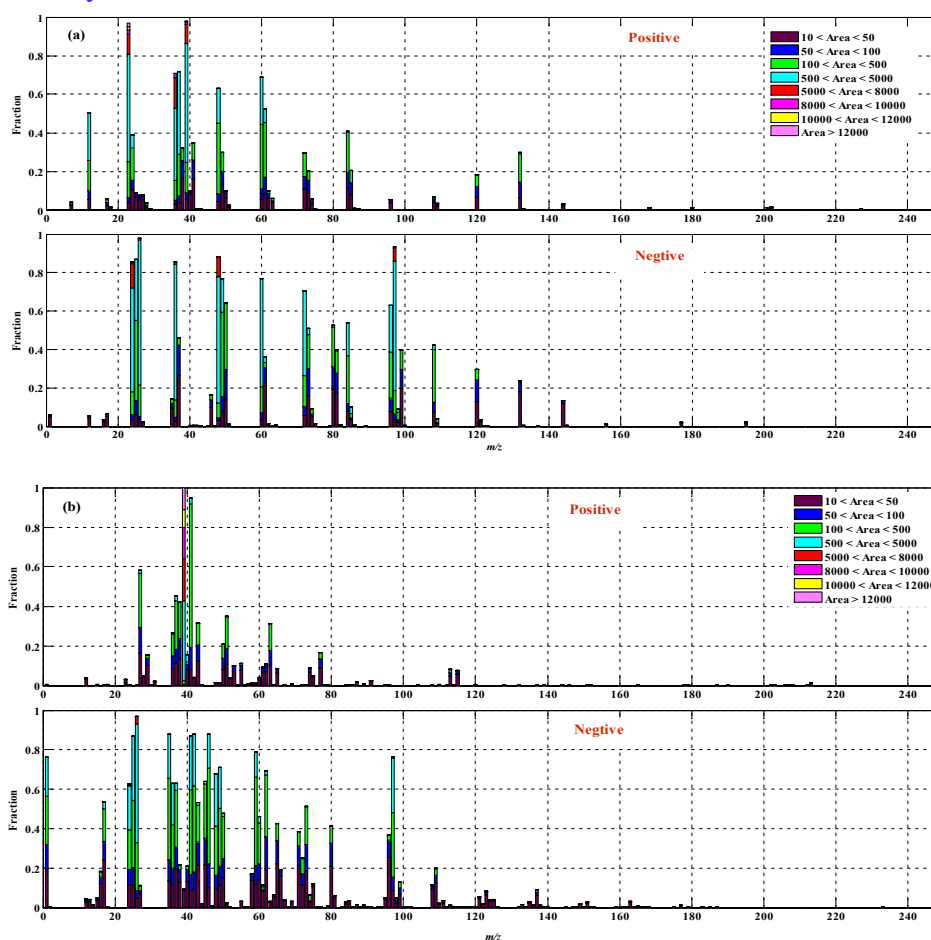
*“Clusters 1, 3, and 4 originated from northeastern Myanmar, accounting for 59.8%, 33.2%, and 4.6% of the total trajectories, respectively.”*

15. Line 257: Again, the discussions of size distributions associated with quantitative results were unreasonable.

**Response:** Thank you for this comment again. The discussions in the main text have been refined. Those changes can be seen in the “tracked change” version of the revised manuscript. The critical revision has been shown in Comment #1.

16. Line 295: High emission of sulfate from coal combustion, biomass burning, and vehicles?

**Response:** The particle mass spectra for coal combustion, biomass burning, and vehicle emissions have strong signals for  $^{97}\text{HSO}_4^-$ . The digitized spectra for coal combustion (Fig. R2a) and biomass burning (Fig. R2b) are obtained from our in-lab experiments. The mass spectrum for vehicular emissions (Fig. Rxxc) was collected by Yang et al (2017). As shown in Fig. R2a, the mass spectra for the coal combustion show strong sulfate ( $^{97}\text{HSO}_4^-$ ) signal, but the nitrate ( $^{62}\text{NO}_3^-$ ) signal is almost absent. As shown in Fig. R2b and c, the mass spectra for biomass burning and vehicular emission contain higher  $^{97}\text{HSO}_4^-$  than  $^{62}\text{NO}_3^-$  signals. The comparison between the mass spectra of the sources and ambient particles sample indicates that the EC-containing particles mainly originated from motor vehicles and coal combustion in our study.



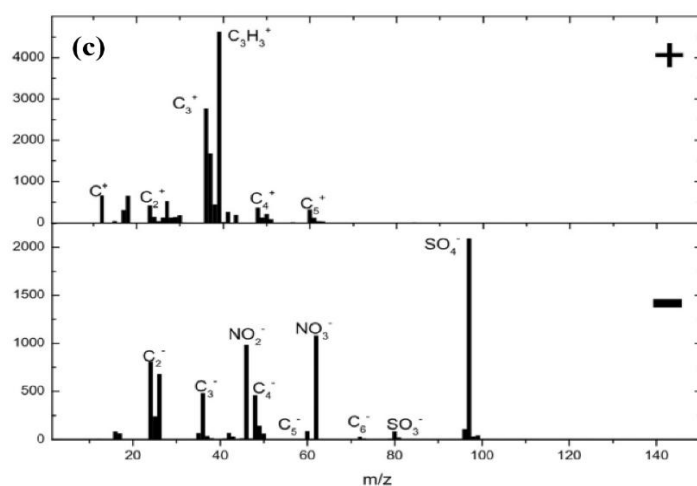


Figure R2. Average digitized spectra for (a) coal combustion and (b) biomass burning emissions obtained with the SPAMS. Vehicle exhaust spectra (c) obtained by Yang et al (2017).

After careful consideration and comparison, the related descriptions have been revised as follows.

Line 329-333:

“Compared to the individual particle mixing state in urban or suburban areas that are located close to emission sources (Chen et al., 2016; Dall'Osto and Harrison, 2012; Zhang et al., 2017a; Li et al., 2022b), the high fractions of sulfate and ammonium at the high altitude area demonstrate a high degree of aging of the individual particles, whereas the low fraction of nitrate with high volatility indicates its loss during transportation processing.”

**Reference:**

Yang, J., Ma, S. X., Gao, B., Li, X. Y., Zhang, Y. J., Cai, J., Li, M., Yao, L.A., Huang, B., Zheng, M.: Single particle mass spectral signatures from vehicle exhaust particles and the source apportionment of on-line PM<sub>2.5</sub> by single particle aerosol mass spectrometry, *Sci. Total Environ.*, 593–594, 310–318, <http://dx.doi.org/10.1016/j.scitotenv.2017.03.099>, 2017.

- Section 3.3: The discussions of Figure 5 and 6 did not show much difference, and the related results were quite similar as Figures 3 and 4. Most part of this section provides little insights into the mixing states of single particles. Authors should add new data analysis and discussions.

**Response:** Sorry for the confusion. Figures 5 and 6 have been transferred from the main text to the Supplementary (new Figures S9 and S10). In addition, the related discussions have been updated in Section 3.2. Moreover, more in-depth elaborations on the mixing states of the single particle are supplemented in Section 3.2 as follows.

Line 305-333:



*“The most abundant of  $^{97}\text{HSO}_4^-$  and  $^{18}\text{NH}_4^+$  fraction are seen in Ammonium (99% and 94%, respectively) and EC-aged (92% and 31%, respectively) particles, whereas much low fraction of  $^{62}\text{NO}_3^-$  is found (2% and 7%, respectively). These suggest that ammonium sulfate is not a predominant form instead of ammonium nitrate (Zhang et al., 2013). The high contribution of sulfate in EC-containing particles also suggests a significant influence of anthropogenically emitted sulfate precursors (e.g.,  $\text{SO}_2$ ) on the aging of EC-containing particles at the high altitude (Peng et al., 2016; Zhang et al., 2017a). Meanwhile, relatively high number fractions of  $^{195}\text{H}(\text{HSO}_4)_2^-$  and  $^{58}\text{C}_2\text{H}_5\text{NHCH}_2^+$  are also observed in Ammonium (63% and 60%) and EC-aged (4% and 19%) particles. These abundant mixtures potentially represent the high hygroscopicity of Ammonium and EC-aged particles, and their ability to neutralize the acidic particles of Ammonium particle (Sorooshian et al., 2007). Then, a moderate fraction of  $^{97}\text{HSO}_4^-$  and  $^{18}\text{NH}_4^+$  are seen on the rich-K (65%, 7%) and OC (56%, 4%) particles. In contrast, more  $^{62}\text{NO}_3^-$  contribute to the rich-K (38%) and OC (68%) particles, mainly affected by vehicle emissions (Text S1). Following BB (18%) and Dust (6%) particles are found in a relatively low number fraction of  $^{97}\text{HSO}_4^-$ , while the moderate  $^{62}\text{NO}_3^-$  accounts for 45% of the BB particle but only 3% of the Dust particle. Besides, the number fraction of  $^{18}\text{NH}_4^+$  is minor (<1%), which suggests the aging degree of BB and Dust particles is relatively low. In addition, oxalate ( $^{89}\text{HC}_2\text{O}_4^-$ ), a representative component of secondary organic formation, is mainly mixed with BB (13%) and rich-K (12%) particles. This is because the substantial precursors of oxalic acid, including acetate ( $^{59}\text{C}_2\text{H}_3\text{O}_2^-$ ), methylglyoxal ( $^{13}\text{C}_3\text{H}_3\text{O}_2^-$ ), glyoxylate ( $^{13}\text{C}_2\text{HO}_3^-$ ), are emitted from biomass burning, while oxalate heterogeneously formed in BB related particles (Ervens et al., 2011). A relatively low fraction (<5%) of the oxalate-containing particles in OC, Ammonium, EC-aged and Dust particles, potentially limited by the contributions of precursor oxalic acid.*

*Compared to the individual particle mixing state in urban or suburban areas that are located close to emission sources (Chen et al., 2016; Dall'Osto and Harrison, 2012; Zhang et al., 2017a; Li et al., 2022b), the high fractions of sulfate and ammonium at the high altitude area demonstrate a high degree of aging of the individual particles, whereas the low fraction of nitrate with high volatility indicates its loss during transportation processing.”*

The impacts of regional transport on the mixing state are further discussed in the revised manuscript as follows.

Line 334-351:

*“The number fractions of six markers in the four clusters were used to further investigate the impacts of regional transport. As shown in Fig. 5a and c, the dominant mixing ion types in each particle (except for Dust type) are similar among the four Clusters. For Cluster 1, the number fractions of  $^{97}\text{HSO}_4^-$  and  $^{89}\text{HC}_2\text{O}_4^-$  have larger values in five particle types (except for Dust type) than those*

*in other clusters. Similar to Cluster 1, 3 and 4 are impacted by regional transport from northeastern Myanmar. Moreover, the fractions of the six markers are similar in OC, Ammonium, and EC-aged types. However,  $^{97}\text{HSO}_4^-$  is decreased in rich-K, BB, and Dust types, while  $^{62}\text{NO}_3^-$  is increased in rich-K and decreased in Dust types. As discussed in Section. 3.1, these phenomena demonstrate that the aging degree of Cluster 3 and 4 might be lower than that of Cluster 1. For Cluster 2, the fraction of  $^{97}\text{HSO}_4^-$  is decreased in rich-K, BB, and EC-aged types but slightly increased in Dust type (Fig. 5f). Such pattern inverse the observations in rich-K, OC, and Dust types for  $^{62}\text{NO}_3^-$  ions. These variations in Cluster 2 are more likely due to influences of biomass-burning activities from the surrounding area of the sampling site, rather than regional transport. Furthermore, Cluster 2 is associated with regional transport from northeastern India along the afternoon to nighttime (from 15:00 LT on May 11<sup>th</sup> to 07:00 LT on 12 May) which is favorable to the nitrate formation  $\text{N}_2\text{O}_5$  by heterogeneous hydrolysis (Wang et al., 2017; Ding et al., 2021). However, these cases are infrequent, as only 2% of trajectories are associated with Cluster 2.”*

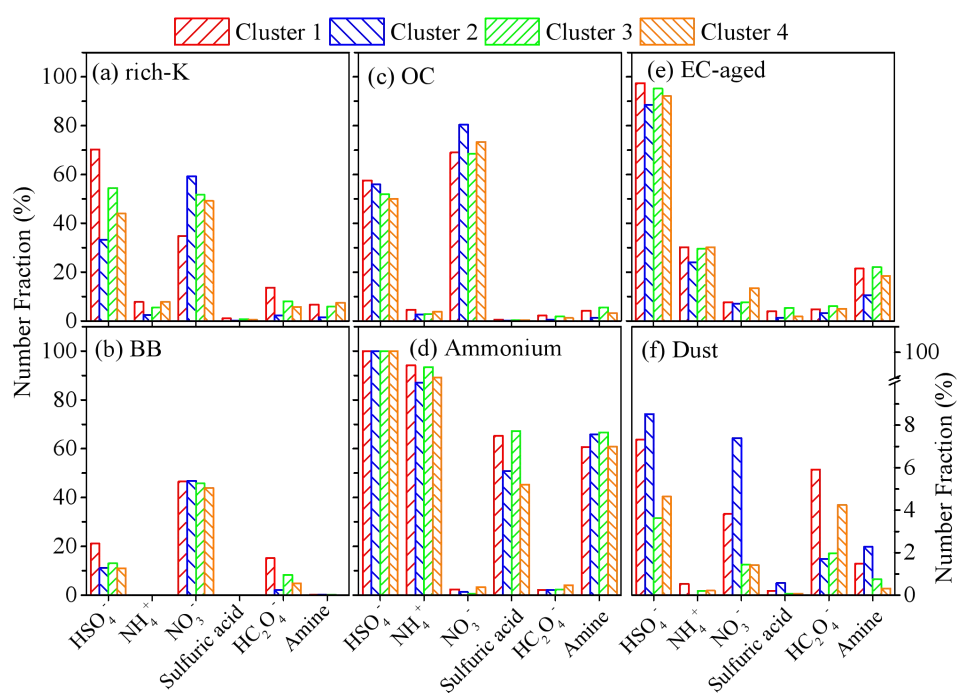


Figure 5. Number fractions of secondary markers associated with the six particle types (i.e., rich-K, BB, OC, Ammonium, EC-aged, and Dust) in four clusters. Secondary markers include sulfate ( $^{97}\text{HSO}_4^-$ ), sulfuric acid ( $^{195}\text{H}(\text{HSO}_4)_2^-$ ), nitrate ( $^{62}\text{NO}_3^-$ ), ammonium ( $^{18}\text{NH}_4^+$ ), amine ( $^{58}\text{C}_2\text{H}_5\text{NHCH}_2^+$ ), and oxalate ( $^{89}\text{HC}_2\text{O}_4^-$ ).

### Reference:

- Zhang, G. H., Bi, X. H., Li, L., Chan, L. Y., Li, M., Wang, X. M., Sheng, G. Y., Fu, J. M., Zhou, Z.: Mixing state of individual submicron carbon-containing particles during spring and fall seasons in urban Guangzhou, China: a case study, *Atmos. Chem. Phys.*, 13(9), 4723–4735, <https://doi.org/10.5194/acp-13-4723-2013>, 2013.
- Zhang, G. H., Han, B. X., Bi, X. H., Dai, S. X., Huang, W., Chen, D. H., Wang, X. M., Sheng, G.

Y., Fu, J. M., Zhou, Z: Characteristics of individual particles in the atmosphere of Guangzhou by single particle mass spectrometry, Atmos. Res., 153, 286–295, <https://doi.org/10.1016/j.atmosres.2014.08.016>, 2015.

18. Line 356-358: “This might be influenced by the pollutant dispersion with the increased PBL height when Ox was evaluated (Fig. S9)”, I don’t think this is a reasonable explanation.

**Response:** Suggestion taken. Relevant contents have been added to explain the opposite linear relationship between secondary aerosol and Ox during E1 and E2 as follows.

Line 377-386:

*“In general, the opposite linear relationship between secondary aerosol and  $O_x$  during E1 and E2 might be influenced by reasons of i) the relatively low secondary formations because of the small amount of precursors emitting from anthropogenic activities around the sampling site (Li et al., 2016); ii) higher dilution rate of the particles formed in the atmosphere with the rapid rise of PBL height during E1 than E2 (Fig. S12a); iii) the degrees of contributions of regional transport due to the low WS ( $0.5 \pm 0.6 \text{ m s}^{-1}$ ) during E1 and the high WS ( $3.1 \pm 1.0 \text{ m s}^{-1}$ ) during E2, respectively (Fig. S8). Therefore, for E1, the increases of  $\text{NO}_3^-$  fraction could be influenced by the local nitrate formation, while the declines of other secondary components should be ascribed to the reduced contribution of regional transport.”*

19. Line 372: The formation of ammonium oxalate was not a correct explanation here.

**Response:** After consideration of this comment, we have made a comparison and provided a comprehensive explanation for the formation of oxalate as follows.

Line 400-405:

*“Considering that the oxalate is abundant mixed in rich-K (14%), BB (15%), EC-aged (5%), and Dust (6%) particles in Cluster 1 (Fig. 5), and the increased contributions of rich-K (39.3%), BB (14.2%) and EC-aged (17.2%) types during E2 (Table 1), the apparent formation of oxalate might be due to the enhancement of regional transport. Particularly, this presents the nearby biomass burning and combustion activities produce more precursor species of oxalate (Sullivan et al., 2007; Kundu et al., 2010; Zhang et al., 2017b).”*

20. Authors didn’t compare the characteristics of single particles with those reported studies in rural and urban areas. This is encouraged to demonstrate the unique mixing states of single particles in TP.

**Response:** Combined those considerations with Comments 17, and 20-21, the explanations on the characteristics of the mixing state in TP have been rewritten. The unique mixing states of individual particles in TP were summarized by gathering the results shown in previous studies in the plain, mountain, and remote areas. The original paragraph has been removed, but the new elaborations have been added in the revised manuscript as follows.

Line 329-333:

*“Compared to the individual particle mixing state in urban or suburban areas that are located close to emission sources (Chen et al., 2016; Dall'Osto and Harrison, 2012; Zhang et al., 2017a; Li et al., 2022b), the high fractions of sulfate and ammonium at the high altitude area demonstrate a high degree of aging of the individual particles, whereas the low fraction of nitrate with high volatility indicates its loss during transportation processing.”*

21. Overall, authors should emphasize the influence of regional transport on the mixing states of single particles in TP, and give more discussions on the aqueous phase and photochemical formation of secondary species in TP.

**Response:** The discussions on the influence of regional transport on mixing states have been added with Comment 17.

Moreover, as the suggestion by the reviewer, more discussions on the aqueous phase and photochemical formation of secondary species in TP are provided in the revised manuscript as follows.

Line 361-440:

*“Photochemical oxidation and aqueous-phase reaction are the key formation pathways of secondary species (Link et al., 2017; Xue et al., 2014; Jiang et al., 2019). Generally, the oxidant  $O_x$  ( $O_3 + NO_2$ ) concentration and RH serve as indicators of the degree of photochemical oxidation (Wood et al., 2010) and aqueous-phase reaction (Ervens et al., 2011). In this study, the relative number fractions of  $^{43}C_2H_3O^+$ ,  $^{89}HC_2O_4^-$ ,  $^{62}NO_3^-$ ,  $^{97}HSO_4^-$ , and  $^{18}NH_4^+$ -containing particles to the total detected particles were selected to indicate the secondary formation (Liang et al., 2022). The correlations of the number fraction of each secondary species with the  $O_x$  concentrations during daytime (from 06:00 to 20:00 LT) and RH during nighttime (from 20:00 to 06:00 next day LT) are used to present the formation pathways during the two episodes (Li et al., 2022).*

*As illustrated in Fig. 6, for E1,  $^{43}C_2H_3O^+$ ,  $^{89}HC_2O_4^-$ ,  $^{97}HSO_4^-$ , and  $^{18}NH_4^+$  show significant negative linear correlations with  $O_x$  ( $p < 0.01$ ), and the correlation strengths range from moderate to strong ( $r = -0.51$  to  $-0.81$ ). However, the  $^{62}NO_3^-$  fraction shows an upward trend with an insignificant correlation ( $r = 0.33$ ,  $p > 0.05$ ) with the increase in  $O_x$  concentration. For E2,  $^{43}C_2H_3O^+$  shows weak correlation with  $O_x$  ( $r = 0.37$ ,  $p > 0.05$ ), but strong correlations with  $^{89}HC_2O_4^-$ ,  $^{97}HSO_4^-$ , and  $^{18}NH_4^+$  ( $r = 0.81\sim 0.92$ ,  $p < 0.01$ ). It should be noted that  $^{62}NO_3^-$*

has a strong negative correlation ( $r = -0.85$ ,  $p < 0.01$ ) with  $O_x$ . In general, the opposite linear relationship between secondary aerosol and  $O_x$  during E1 and E2 might be influenced by reasons of i) the relatively low secondary formations because of the small amount of precursors emitting from anthropogenic activities around the sampling site (Li et al., 2016); ii) higher dilution rate of the particles formed in the atmosphere with the rapid rise of PBL height during E1 than E2 (Fig. S12a); iii) the degrees of contributions of regional transport due to the low WS ( $0.5 \pm 0.6 \text{ m s}^{-1}$ ) during E1 and the high WS ( $3.1 \pm 1.0 \text{ m s}^{-1}$ ) during E2, respectively (Fig. S8). Therefore, for E1, the increases of  $\text{NO}_3^-$  fraction could be influenced by the local nitrate formation, while the declines of other secondary components should be ascribed to the reduced contribution of regional transport. For E2, the decreased  $\text{NO}_3^-$  fraction could be caused by the relatively higher volatilization loss of nitrate than other components through the regional transport. Previous study proves that the formations of organic nitrate species (such as  $^{27}\text{CHN}^+$ ,  $^{30}\text{NO}^+$ ,  $^{43}\text{CHO}_1\text{N}^+$  and  $\text{CHO}_x\text{N}^+$ ) through the  $\text{NO} + \text{RO}_2$  pathway dominate 80% of the total nitrate production in tropical forested regions during summertime (Alexander et al., 2009). Aruffo et al (2022) also found that low  $\text{NO}_x$  concentration (i.e.  $< 6 \text{ ppbv}$ ), compared to  $2.3 \pm 0.8 \text{ ppbv}$  in this study, could even promote the particle-phase partitioning of the lower volatility of organonitrates. These results suggest that photo-oxidation reactions could promote the secondary formation, among which the rate of  $\text{HSO}_4^-$  formation (slop = 0.017) is the highest. Increased with  $O_x$  concentration during E2, the concentration levels of secondary organic species of  $\text{C}_2\text{H}_3\text{O}^+$  (18-28%) imperceptibly rise, while the oxalate fraction significantly increase by 7-20% as well. The results indicate that the secondary organic species have different formation capacities through atmospheric oxidation.

Considering that the oxalate that is abundant mixed in rich-K (14%), BB (15%), EC-aged (5%), and Dust (6%) particles in Cluster 1 (Fig. 5), and the increased contributions of rich-K (39.3%), BB (14.2%) and EC-aged (17.2%) types during E2 (Table 1), the apparent formation of oxalate might be due to the enhancement of regional transport. Particularity, this presents the nearby biomass burning and combustion activities produce more precursor species of oxalate (Sullivan et al., 2007; Kundu et al., 2010; Zhang et al., 2017b).

Fig. 7 illustrates that the number fractions of  $^{43}\text{C}_2\text{H}_3\text{O}^+$ ,  $^{89}\text{HC}_2\text{O}_4^-$ ,  $^{97}\text{HSO}_4^-$ , and  $^{18}\text{NH}_4^+$  have moderate to strong positive correlations with RH ( $r = 0.70\sim 0.81$ ,  $p < 0.01$  or  $0.05$ ) in the nighttime during the two episodes, except that  $^{43}\text{C}_2\text{H}_3\text{O}^+$  during E2 ( $p = 0.48$ ) and  $^{89}\text{HC}_2\text{O}_4^-$  during E1 ( $p = 0.12$ ). Furthermore,  $^{62}\text{NO}_3^-$  fraction has no obvious changes with insignificant correlation with RH during E1 ( $p = 0.43$ ) and presents a moderate negative correlation with RH ( $r = 0.69$ ,  $p < 0.01$ ) during E2. As shown in Fig. 7e, the highest aqueous formation rate of  $\text{HSO}_4^-$  is mainly due to the properties of low volatile and high hygroscopic sulfate (Wang et al., 2016; Zhang et al., 2019c; Sun et al., 2013). Compared with that during E2 (slop=0.014), the decreased formation rate of  $\text{HSO}_4^-$  during the E1 (slop=0.009) may be because of the decreases of aerosol acidity in higher

*RH > 80% (Huang et al., 2019; Meng et al., 2014; Tian et al., 2021). And the increased contributions of regional transport due to the high WS ( $2.4 \pm 0.8 \text{ m s}^{-1}$ ) during E2 are comparable to the low WS ( $0.08 \pm 0.08 \text{ m s}^{-1}$ ) during E1 (Fig. S8). The fair production rate of  $\text{NH}_4^+$  during the E1 (slop=0.005) and E2 (slop=0.006) demonstrate that an aqueous-phase reaction could effectively promote ammonium formation. Meanwhile, a slightly larger slop during E2 could be also affected by the increased contributions of regional transport. Compared with those during E1, the inverse generation rates of two secondary organic species (i.e.,  $\text{C}_2\text{H}_3\text{O}^+$  and  $\text{HC}_2\text{O}_4^-$ ) during E2 are possibly caused by the different formation pathways with a variety of RH levels or distinct regional transports. For example,  $\text{C}_2\text{H}_3\text{O}^+$  shows a strong correlation with RH ( $r = 0.70$ ,  $p < 0.05$ ) during E1 (slop=0.003) but has an insignificant correlation during E2. This could be explained by high RHs that could effectively promote secondary organic formation during E1. In addition, the  $\text{HC}_2\text{O}_4^-$  fraction increases slightly (9.7-13.1%) during E1 is potentially ascribed to more abundant Dust-type particles (20.3%) which compose of high calcium (Fig. S13) that favor the formation of metal oxalate complexes (i.e., Ca oxalate). At high RHs ( $93.4 \pm 7.6\%$ ), if oxalate ions are dissolved in the aqueous phase with the presence of Ca ions, the Ca oxalate complexes can precipitate because of their low hygroscopic and insoluble natures (Furukawa and Takahashi, 2011). This could offset the oxalate formation in the aqueous-phase reaction. However, significant linear increases (slop=0.003) with RH ( $r = 0.81$ ,  $p < 0.01$ ) during E2 demonstrate that the aqueous-phase reaction effectively promotes the oxalate formation (Cheng et al., 2017; Meng et al., 2020). No obvious change and insignificant correlation between  $^{62}\text{NO}_3^-$  and RH are found during E1, potentially attributed to the decreases of  $\text{NO}_2$  concentration ( $3.7 \pm 0.4 \text{ ppbv}$ ) in the local atmosphere. Meanwhile, high RHs could promote organonitrates formation (Fang et al., 2021; Fry et al., 2014). The linearity between  $^{62}\text{NO}_3^-$  and RH ( $r = 0.69$ ,  $p < 0.01$ ) significantly decreases during E2, mostly due to the losses of the volatile compound through the regional transport (Fig. S14)."*